

Copper and Nitrogen Co-Doping Effect on Visible-Light Responsive Photocatalysis of Plasma-Nitrided Copper-Doped Titanium Oxide Film

Ken-Ichi Hirota, Masahiko Maeda

College of Engineering, Kanazawa Institute of Technology, Ishikawa, Japan

Email: mmaeda@neptune.kanazawa-it.ac.jp

How to cite this paper: Hirota, K.-I. and Maeda, M. (2017) Copper and Nitrogen Co-Doping Effect on Visible-Light Responsive Photocatalysis of Plasma-Nitrided Copper-Doped Titanium Oxide Film. *Journal of Materials Science and Chemical Engineering*, 5, 52-62.

<https://doi.org/10.4236/msce.2017.512005>

Received: November 30, 2017

Accepted: December 24, 2017

Published: December 27, 2017

Copyright © 2017 by authors and Scientific Research Publishing Inc.

This work is licensed under the Creative Commons Attribution International License (CC BY 4.0).

<http://creativecommons.org/licenses/by/4.0/>



Open Access

Abstract

In order to clarify the visible-light responsive photocatalysis of TiO₂ co-doped with Cu and N atoms, plasma-nitridation was taken place to Cu-doped TiO₂ film. Cu-doped TiO₂ films were prepared by dip-coating method and they were nitrided by nitrogen plasma in the plasma-enhanced CVD system. Cu-doped TiO₂ films before and after plasma-nitridation show similar X-ray diffraction peaks of anatase TiO₂. XPS analysis reveals that the ionic states of Ti and Cu in the Cu-doped TiO₂ films are Ti⁴⁺ and Cu⁺, respectively. After nitrogen plasma treatment, oxygen atoms are released by substitution of nitrogen atoms in the TiO₂ matrix, so that Cu⁺ is oxidized to generate Cu²⁺ and at the same time oxygen vacancy is formed. The absorption edge of both Cu-doped and plasma-nitrided Cu-doped TiO₂ did red shift. Visible-light responsive photocatalytic activity of the Cu-doped TiO₂ film degraded after nitrogen plasma treatment.

Keywords

Sol-Gel, Cu-Doped Titania, Plasma-Nitridation, Photocatalysis

1. Introduction

Titanium dioxide (TiO₂) is well known as chemically stable and harmless material, and has been applied widely in various fields such as photocatalysts [1] [2] [3], dye-sensitized solar cells [4] [5] [6], water splitting [3] [7], and so on. In recent years, it has been received a great deal of attention especially as an environmental purification materials, because of its photocatalytic decomposition of

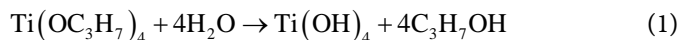
persistent organic pollutants, and photo-induced hydrophilicity [8] [9] [10] [11]. Various utilizations such as antibacterial, antipollution and deodorization have been attained. Because of these unique photocatalytic properties, application of the TiO₂ will spread increasingly from now on. However, ultraviolet-light irradiation is necessary to fulfill its photocatalytic functions, so the TiO₂ photocatalyst is holding many problems including a limitation of application range and utilization efficiency of light. In order to improve the photocatalytic efficiency and to expand the application range, development of the visible-light responsive photocatalyst is demanded.

Visible-light responsive photocatalysts have been studied extensively using various kinds of approach. Among them, doping of transition metal cations or non-metal anions into the TiO₂ lattice has shown promising results in improving the visible-light response of TiO₂ photocatalysts [12]-[18].

This paper describes the effect of plasma-nitridation on visible-light responsive photocatalysis of Cu-doped TiO₂ films. The nitrogen atoms introduced into the Cu-doped TiO₂ matrix by plasma-nitridation substitute to the oxygen sites, and oxygen atoms release from the TiO₂ matrix. As a result, Cu²⁺ in CuO increases due to oxidation of Cu⁺ in Cu₂O. At the same time, oxygen vacancies are formed. The visible-light response of photocatalysis is observed in the Cu-doped TiO₂ film, however, it degrades after nitrogen-plasma treatment. It is considered that the both Cu²⁺ and oxygen vacancy act as recombination center of electrons and holes.

2. Experimental

The Cu-doped TiO₂ films were prepared by dip-coating using sol solution mixed titanium tetraisopropoxide, ethanol, hydrochloric acid, water, and metallic salt. The procedure of preparation of the sol solution was as follows; the mixture of titanium tetraisopropoxide (TTIP) and ethanol (C₂H₅OH) was stirred for 2 hours, and copper (II) chloride dihydrate (CuCl₂·2H₂O) was dissolved in the mixture of C₂H₅OH, deionized water (H₂O), and hydrochloric acid (HCl) and also stirred for 2 hours, after then both solutions were mixed and stirred for more 2 hours. The ratio of each reagent was TTIP:C₂H₅OH:H₂O:HCl = 1:5:5:0.4, and 2 mol% of metallic salt against TTIP was added in case of deposition for the Cu-doped TiO₂ films. The flow of preparation of the sol solution is shown in **Figure 1**. In the sol-gel reaction using TTIP as a raw material, TiO₂ is formed by a hydrolysis reaction and a condensation-polymerization reaction as shown in Equations (1) and (2). In the case of doping Cu atoms, it is taken into TiO₂ in the monovalent or divalent oxidation state during the sol-gel reaction.



The substrate used was Si wafer. In case of transmission spectra measurements, quartz substrate was used. Dip-coating and pre-annealing at 120 °C for 10 min were

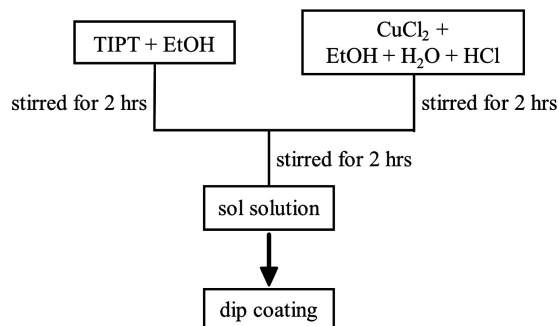


Figure 1. The flow of preparation of the sol solution.

repeated three times and then post-annealed at 500°C for 30 min. Withdrawal speed was 2 mm/sec.

After post-annealing, film thickness was about 200 nm. All heat treatments were carried out under nitrogen ambient. **Figure 2** shows the capacitance coupled plasma-enhanced CVD equipment which uses a high frequency of 13.56 MHz. In this work, nitrogen gas was used for the plasma-nitridation. Flow rate of nitrogen gas was kept constant of 100 sccm. RF power, substrate temperature, and gas pressure were 100 W, 350°C, and 133 Pa, respectively. Plasma-nitridation was carried out for the sol-gel derived Cu-doped TiO₂ films after post-annealing. Characterizations of the deposited films were carried out by Atomic force microscopy (AFM; Shimazu SPM-9700), X-ray diffraction (XRD; RIGAKU RINT-2100, CuK α X-ray source operating at 30 kV and 20 mA), X-ray photoelectron spectroscopy (XPS; PHI ESCA-1600, AlK α X-ray source operating at 400 W), and optical absorption spectroscopy (UV-Vis; Ocean Optics USB2000), respectively.

Photocatalytic activities of the Cu-doped TiO₂ films deposited on quartz substrate before and after plasma-nitridation were evaluated by pigment degradation measurement. The fluorescent light with UV-cut filter (<420 nm) was used for visible-light sources. The degradation rate of methylene blue as a pigment was evaluated by measuring the changes in absorbance of 654 nm using UV-Vis spectrometer. The films were soaked in the 1 mmol/L methylene blue solution for 60 min, and then the samples were dried in the dark after the methylene blue on the back surface was wiped off. The absorbance at 654 nm was measured every 15 min visible-light irradiation.

3. Results and Discussion

3.1. Depth Profile of Nitrogen Atoms

Nitrogen distribution in the plasma-nitrided Cu-doped film was evaluated by XPS, and depth profile of nitrogen atoms was shown in **Figure 3**. During XPS measurements, the film was step-etched in 2% HF solution. The vertical axis shows normalized N1s peak intensity against the film before step-etching. Almost all the nitrogen atoms exist within 30 - 40 nm of surface region. It is considered that the nitridation takes place only around the surface region, because

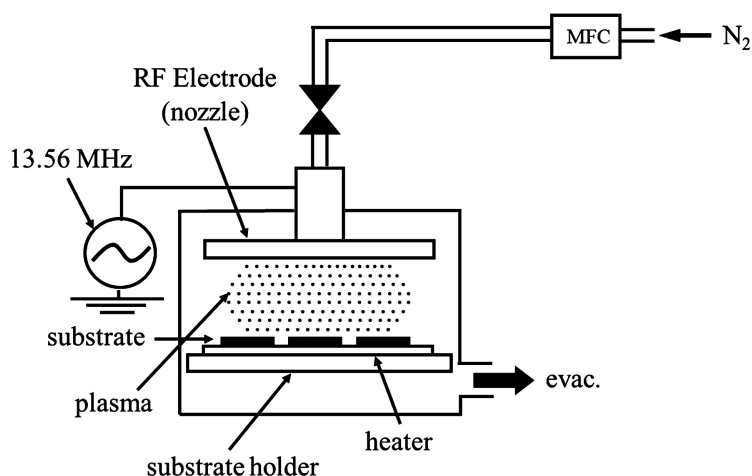


Figure 2. Schematic of the capacitance coupled plasma-enhanced CVD equipment.

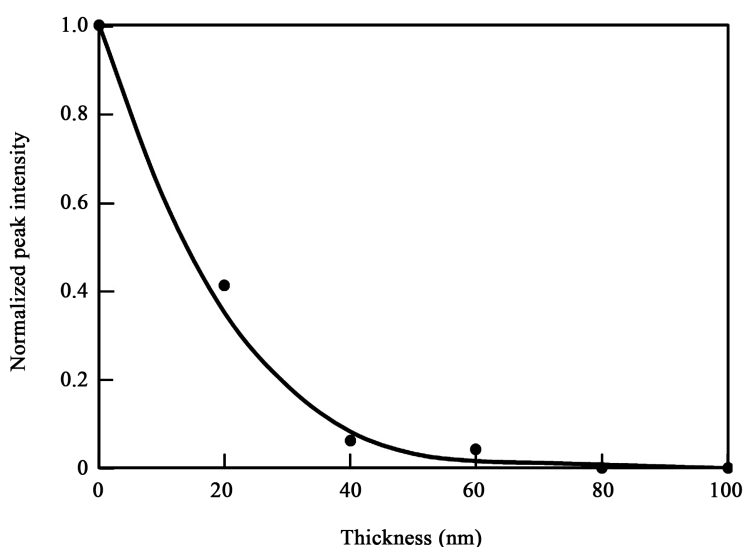


Figure 3. Depth profile of nitrogen atoms in plasma-nitrided Cu-doped TiO_2 film.

structure of the plasma-nitrided film becomes dense after post-annealing at 500°C for 30 min.

3.2. Structural Evaluation of the Films

Figure 4 shows the AFM image of the surface morphology of the Cu-doped TiO_2 film after post-annealing at 500°C for 30 min. Surface shape with fine dense particles of several tens of nanometers in diameter and about 30 nm in height are observed. There was no significant difference in the surface shape after the nitrogen plasma treatment. The crystalline structure of the films was evaluated by XRD. The X-ray diffraction patterns for the non-doped, Cu-doped and plasma-nitrided Cu-doped TiO_2 films are shown in **Figure 5**. All the films show the diffraction peaks of anatase (101), (112), and (200) of TiO_2 with each same intensities. It is found that the crystallization of the TiO_2 is hardly affected by Cu doping and nitrogen-plasma treatment.

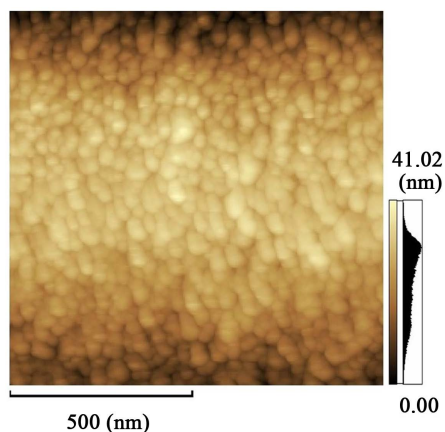


Figure 4. Surface morphology of the Cu-doped TiO₂ film.

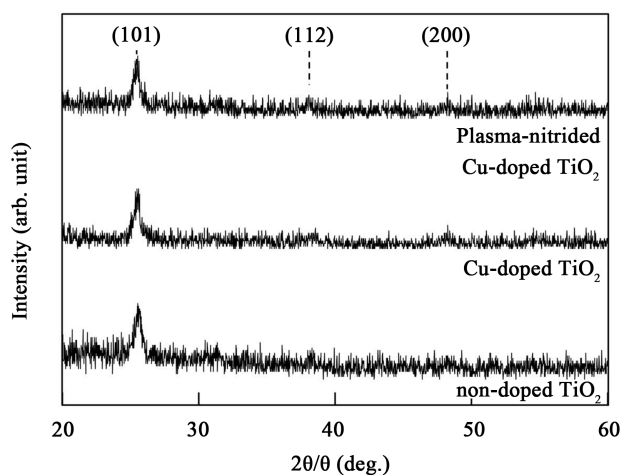


Figure 5. X-ray diffraction patterns for the non-doped, Cu-doped, and plasma-nitrided Cu-doped TiO₂ films.

The film composition was analyzed by XPS. The XPS spectra of Ti2p, O1s, and Cu2p electrons of the Cu-doped TiO₂ film are shown in **Figure 6**. Ti2p_{3/2} and Ti2p_{1/2} electrons have peaks at binding energies of 458.7 eV and 464.3 eV, respectively, which implies that the ionic state of titanium is Ti⁴⁺ [19]. The prominent sharp O1s peak at 529.9 eV is associated with the oxygen of TiO₂ [20]. The Cu2p_{3/2} peak at 932.2 and Cu2p_{1/2} peak at 952.1 eV are both assigned to Cu⁺ [20].

The XPS spectra of the plasma-nitrided Cu-doped TiO₂ film are shown in **Figure 7**. Ti2p signals are hardly changed compared with those of the Cu-doped TiO₂ film, however, O1s of N-O bonds at 531.3 eV, and N1s of Ti-N bonds at 397.1 eV are observed [15].

Moreover, two peaks at 934.5 eV (Cu2p_{3/2}) and 954.7 eV (Cu2p_{1/2}), assigned to Cu²⁺ are obviously observed as shown in **Figure 6(d)** [20].

In the Cu-doped TiO₂ films, Cu exists as Cu₂O in the nearly stoichiometric TiO₂ matrix and its content is estimated about 2 at% by calculation using sensitivity factor. When the Cu-doped TiO₂ films are treated in the nitrogen-plasma,

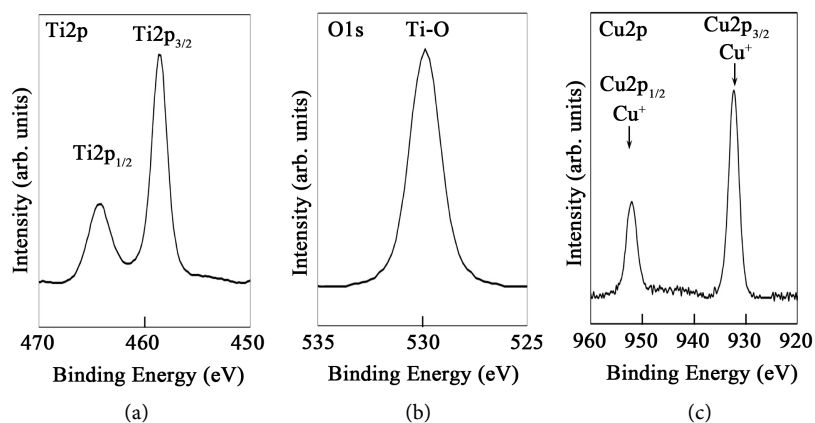


Figure 6. The XPS spectra of (a) Ti2p; (b) O1s; and (c) Cu2p electrons of Cu-doped TiO₂ film.

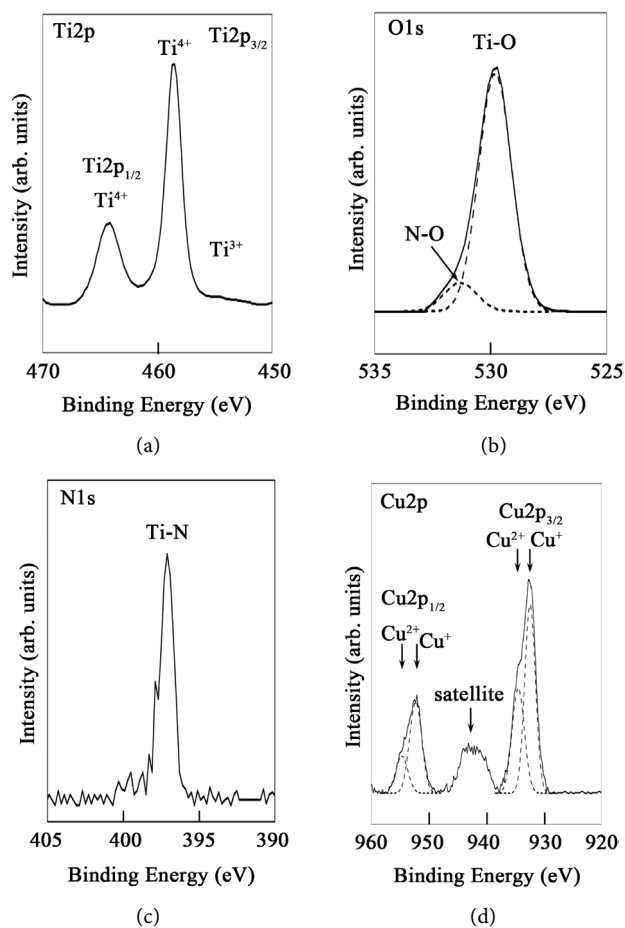


Figure 7. The XPS spectra of (a) Ti2p; (b) O1s; (c) N1s; and (d) Cu2p electrons of plasma-nitrided Cu-doped TiO₂ film.

introduced nitrogen atoms replace the oxygen sites and oxygen atoms release from the TiO₂ matrix, as a result, a part of Cu⁺ is oxidized and changes to Cu²⁺. At a same time, oxygen vacancies are considered to be formed in the TiO₂ matrix.

3.3. Visible-Light Responsive Photocatalysis

Figure 8 shows transmission spectra of non-doped TiO₂, Cu-doped TiO₂, and plasma-nitrided Cu-doped TiO₂ films, respectively. The absorption edges of Cu-doped TiO₂ and plasma-nitrided Cu-doped TiO₂ films do red shift compared with that of non-doped TiO₂ film. Slightly large red shift is observed with the plasma-nitrided Cu-doped TiO₂ film.

Bandgap energies of TiO₂, Cu₂O, and CuO are 3.2, 2.1, and 1.76 eV, respectively [21]. So, visible-light absorption of the Cu-doped TiO₂ is due to Cu₂O exist in the film. In case of the plasma-nitrided Cu-doped TiO₂, oxidation state of a part of Cu₂O changes to CuO, and in addition, bandgap of TiO₂ decreases because of replacement of O atoms with N atoms in the TiO₂ matrix, as a result visible-light absorption enhances compared with the Cu-doped TiO₂.

The visible-light responsive photocatalysis was evaluated by measuring degradation of methylene blue using UV-Vis spectroscopy. **Figure 9** shows the transmittance of methylene blue solution at 654 nm as a function of visible-light irradiation time. The transmittance decreases exponentially with increase of the irradiation time in both cases of the Cu-doped TiO₂ and plasma-nitrided Cu-doped TiO₂ films.

Assuming that the decomposition reaction of methylene blue is the first-order reaction, the natural logarithm of the transmittance ratio, *i.e.* absorbance, before and after irradiation as a function of the irradiation time is shown in **Figure 10**. In both cases, linear relationship is shown and the rate constant that is calculated by the gradient of the linear line of the plasma-nitrided Cu-doped TiO₂ film decreases to about 60% of the Cu-doped TiO₂ film.

Conduction band edges of TiO₂, Cu₂O, and CuO are 0.21, 0.75, and -0.50 V (vs. NHE), respectively [21]. In the Cu-doped TiO₂, excited electrons into the conduction band of Cu₂O by visible-light irradiation diffuse to the conduction

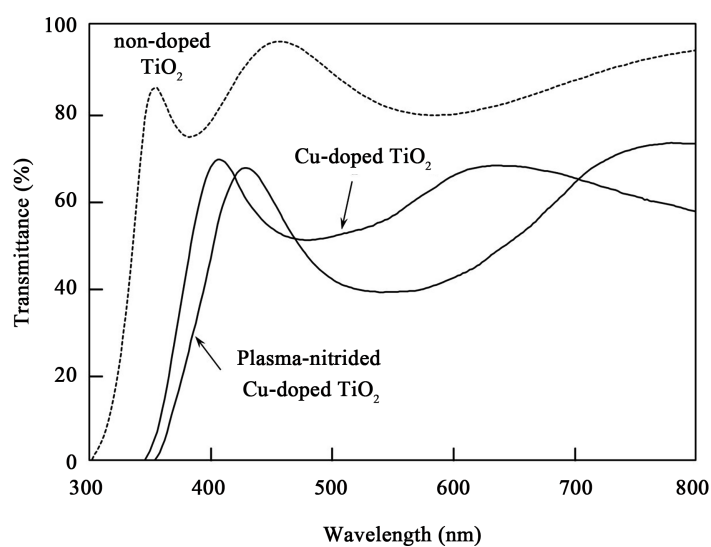


Figure 8. Transmission spectra of non-doped TiO₂, Cu-doped TiO₂, and plasma-nitrided Cu-doped TiO₂ films.

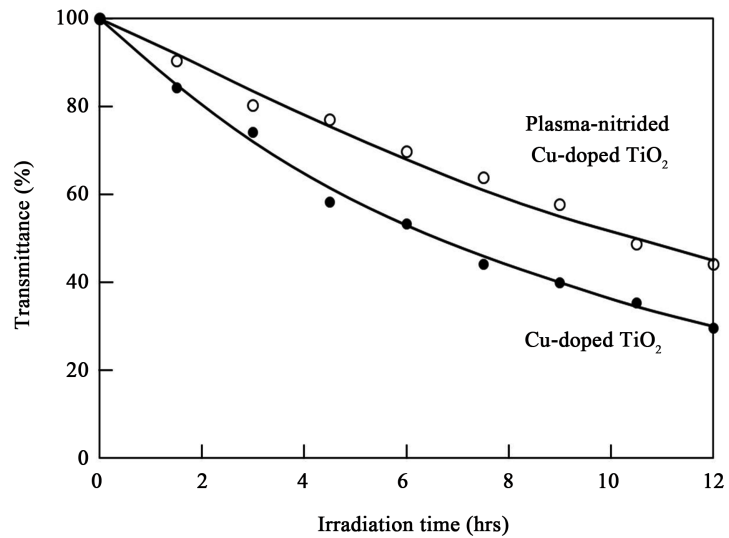


Figure 9. Transmittance of methylene blue solution at 654 nm as a function of visible-light irradiation time.

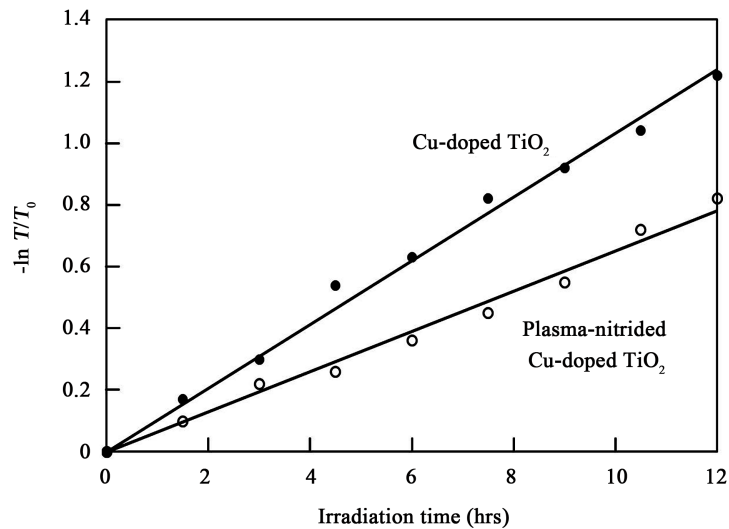


Figure 10. Natural logarithm of the absorbance ratio before and after visible-light irradiation as a function of the irradiation time.

band of the TiO₂, the visible-light responsive photocatalysis is observed. In case of the plasma-nitrided Cu-doped TiO₂, however, it is considered that impurity level of CuO formed in the bandgap of the TiO₂, and oxygen vacancy due to break of Ti-O bonds by plasma-treatment act as recombination center. As a result, photocatalytic activity degrades.

The Cu doping into the TiO₂ films is effective for the visible-light responsive photocatalysis, however, the nitrogen-plasma treatment of the Cu-doped TiO₂ film leads to formation of impurity level and oxygen vacancy. Because these act as recombination centers of carriers, the Cu and N atoms co-doping effect for enhancement of visible-light photocatalysis using nitrogen plasma treatment of the Cu-doped TiO₂ film was not observed unfortunately.

4. Conclusions

Copper and nitrogen co-doping effect on visible-light responsive photocatalysis of plasma-nitrided copper-doped titanium oxide film was investigated.

Cu exists as Cu_2O in the nearly stoichiometric TiO_2 matrices, and the crystallinity of TiO_2 is hardly affected by Cu doping. The absorption edge of the Cu-doped TiO_2 film did red shift compared with that of non-doped TiO_2 film, it is due to Cu_2O with bandgap of 2.1 eV. When the Cu-doped TiO_2 film was treated in nitrogen plasma, oxidation state of a part of Cu_2O changes to CuO , and in addition, bandgap of TiO_2 decreases because of replacement of O atoms with N atoms in the TiO_2 matrix, as a result, visible-light absorption enhances compared with the Cu-doped TiO_2 . The visible-light responsive photocatalysis of the Cu-doped TiO_2 film is due to excited electrons to the conduction band of Cu_2O by visible-light irradiation diffuse to conduction band of TiO_2 . In the plasma-nitrided Cu-doped TiO_2 , it is considered that both the Cu^{2+} formed by oxidation of Cu^+ and oxygen vacancy act as recombination centers, as a result, photocatalytic activity degrades.

In this study, it is found that oxygen atoms were released from TiO_2 in the plasma-nitridation process of the Cu-doped TiO_2 , and leads to formation of impurity level and oxygen vacancy, as a result, the photocatalytic activity degraded. In order to suppress release of oxygen atoms, it is considered that using of mixed gas plasma of oxygen and nitrogen gases is effective.

Acknowledgements

The authors would like to thank Mrs. Yaoyama T and Watanabe T for their experimental assistance.

References

- [1] Rashidi, S., Nikazar, M., Yazdi, A.V. and Fazaeli, R.J. (2014) Optimized Photocatalytic Degradation of Reactive Blue 2 by TiO_2 /UV Process. *Environmental Science and Health, Part A*, **49**, 452-462. <https://doi.org/10.1080/10934529.2014.854685>
- [2] Lin, H., Huang, C.P., Li, W., Ni, C., Shah, S.I. and Tseng, Y.H. (2006) Size Dependency of Nanocrystalline TiO_2 on its Optical Property and Photocatalytic Reactivity Exemplified by 2-Chlorophenol. *Applied Catalysis B Environmental*, **68**, 1-11. <https://doi.org/10.1016/j.apcatb.2006.07.018>
- [3] Ni, M., Leung, M.K.H., Leung, D.Y.C. and Sumathy, K. (2007) A Review and Recent Developments in Photocatalytic Water-Splitting Using TiO_2 for Hydrogen Production. *Renewable and Sustainable Energy Review*, **11**, 401-425. <https://doi.org/10.1016/j.rser.2005.01.009>
- [4] O'Regan B. and Grätzel, M. (1991) A Low-Cost, High-Efficiency Solar Cell Based on Dye-Sensitized Colloidal TiO_2 films. *Nature*, **353**, 737-740. <https://doi.org/10.1038/353737a0>
- [5] Kim, D.H., Seong, W.M., Park, I.J., Yoo, E.S., Shin, S.S., Kim, J.S., Jung, H.S., Lee, S. and Hong, K.S. (2013) Anatase TiO_2 Nanorod-Decoration for Highly Efficient Photoenergy Conversion. *Nanoscale*, **5**, 11725-11732. <https://doi.org/10.1039/c3nr03439a>

- [6] Kuzmych, O., Nonomura, K., Johansson, E.M.J., Nyberg, T., Hagfeldt, A. and Skompska, M. (2012) Defect Minimization and Morphology Optimization in TiO₂ Nanotube Thin Films, Grown on Transparent Conducting Substrate, for Dye Synthesized Solar Cell Application. *Thin Solid Films*, **522**, 71-78. <https://doi.org/10.1016/j.tsf.2012.09.011>
- [7] Fujishima, A. and Honda, K. (1972) Electrochemical Photolysis of Water at a Semiconductor Electrode. *Nature*, **238**, 37-38. <https://doi.org/10.1038/238037a0>
- [8] Li, L., Wei, L., Yuexiang, Z., Biying, Z. and Youchang, X. (2005) Phosphor-Doped Titania - A Novel Photocatalyst Active in Visible Light. *Chemistry Letters*, **34**, 284-285. <https://doi.org/10.1246/cl.2005.284>
- [9] Shannon, M.A., Bohn, P.W., Elimelech, M., Georgiadis, J.G., Mariñas, B.J. and Mayes, A.M. (2008) Science and Technology for Water Purification in the Coming Decades. *Nature*, **452**, 301-310. <https://doi.org/10.1038/nature06599>
- [10] Zhang, T., Zhang, X., Ng, J., Yang, H., Liu, J. and Sun, D.D. (2.11) Fabrication of Magnetic Cryptomelane-Type Manganese Oxide Nanowires for Water Treatment. *Chemical Communications*, **47**, 1890-1892. <https://doi.org/10.1039/C0CC03265D>
- [11] Wang, R., Hashimoto, K., Fujishima, A., Chikumi, M., Kojima, E., Kitamura, A., Shimohigoshi, M. and Watanabe, T. (1977) Light-Induced Amphiphilic Surfaces. *Nature*, **388**, 431-432. <https://doi.org/10.1038/41233>
- [12] Colón, G., Maicu, M., Hidalgo, M.C. and Navío, J.A. (2006) Cu-Doped TiO₂ Systems with Improved Photocatalytic Activity. *Applied Catalysis B: Environmental*, **67**, 41-51. <https://doi.org/10.1016/j.apcatb.2006.03.019>
- [13] Nakano, T., Kogoshi, S. and Katayama, N. (2015) Cu-Supported TiO₂ with High Visible-Light Photocatalytic Activity Prepared Using Cupric Acetate. *e-Journal of Surface Science and Nanotechnology*, **13**, 143-146. <https://doi.org/10.1380/ejssnt.2015.143>
- [14] Zhou, J., Takeuchi, M., Ray, A.K., Anpo, M. and Zhao, X. (2007) Enhancement of Photocatalytic Activity of P25 TiO₂ by Vanadium-Ion Implantation under Visible Light Irradiation. *Journal of Colloid and Interface Science*, **311**, 497-501. <https://doi.org/10.1016/j.jcis.2007.03.007>
- [15] Asahi, R., Morikawa, T., Ohwaki, T., Aoki, T. and Taga, Y. (2001) Visible-Light Photocatalysis in Nitrogen-Doped Titanium Oxides. *Science*, **293**, 269-271. <https://doi.org/10.1126/science.1061051>
- [16] Zhang, J.L., Wu, Y.M., Xing, M.Y., Lenghari, S.A.K. and Sajjad, S. (2010) Development of Modified N Doped TiO₂ Photocatalyst with Metals, Nonmetals and Metal Oxides. *Energy Environmental Science*, **3**, 715-726. <https://doi.org/10.1039/b927575d>
- [17] Ohno, T., Mitsui, T. and Matsumura, M. (2003) Photocatalytic Activity of S-Doped TiO₂ Photocatalyst under Visible Light. *Chemistry Letters*, **32**, 364-365. <https://doi.org/10.1246/cl.2003.364>
- [18] Murakami, Y., Kasahara, B. and Nosaka, Y. (2007) Photoelectrochemical Properties of the Sulfur-Doped TiO₂ Film Electrodes: Characterization of the Doped States by Means of the Photocurrent Measurements. *Chemistry Letters*, **36**, 330-331. <https://doi.org/10.1246/cl.2007.330>
- [19] Pham T.D. and Lee, B.K. (2014) Cu Doped TiO₂/GF for Photocatalytic Disinfection of Escherichia coli in bioaerosols under Visible Light Irradiation: Application and Mechanism. *Applied Surface Science*, **296**, 15-23. <https://doi.org/10.1016/j.apsusc.2014.01.006>

- [20] Sreekantan, S., Zaki, S.M., Lai, C.W. and Tzu, T.W. (2014) Copper-Incorporated Titania Nanotubes for Effective Lead Ion Removal. *Materials Science in Semiconductor Processing*, **26**, 620-631. <https://doi.org/10.1016/j.mssp.2014.05.034>
- [21] Wang, P., Wen, X., Amal, R. and Ng, Y.H. (2015) Introducing a Protective Interlayer of TiO₂ in Cu₂O-CuO Heterojunction Thin Film as a Highly Stable Visible Light Photocathode. *RSC Advances*, **5**, 5231-5236. <https://doi.org/10.1039/C4RA13464H>